

# CONTRIBUTION TO THERMAL ANALYSIS OF THE AIR-COOLED PEM FUEL CELL

Viktor Ferencey, Michal Stromko, Kristián Ondrejčka

## **Abstract:**

---

*This contribution deals with thermal modelling and experimental analysis of the air-cooled PEM (Proton Exchange Membrane) fuel cell for power systems of transportation applications. The technology of the energy conversion which directly converts chemical energy of the fuel (hydrogen fuel) into electrical energy presents a potential replacement for the conventional internal combustion engine (ICE) in transportation applications. PEM fuel cell is an electrochemical energy conversion device which converts chemical energy of hydrogen and oxygen directly and efficiently into electrical energy with waste heat and liquid water as by-products of the reaction. There is a number of advantages to a PEM fuel cell powered electromobility that use hydrogen such as energy efficient and environmentally benign low temperature operation, quick start-up, compatibility with renewable energy sources and ability to obtain a power density competitive with the internal combustion engine in the perspective. This paper explores the limits of using the air cooling for Polymer Electrolyte Membrane (PEM) stacks. Thermal analysis of the air-cooled fuel cells is, however, a major problem that stems from a low operating temperatures of PEM fuel cell stacks in contrast to the conventional internal combustion engines. In the present study, a numerical thermal model is presented in order to analyse the heat transfer and predict the temperature distribution in air-cooled PEM fuel cells. In order to validate the performance of the created analytical simulation model, comparisons of the data obtained through experimental measurements in the Fuel Cells laboratory have been made.*

## **Keywords:**

*PEM fuel cells, power system, thermal engineering, temperature, heat transfer, air cooling, hydrogen fuel, electrochemical device, conversion, temperature distribution.*

## **ACM Computing Classification System:**

*Temperature simulation and estimation, renewable energy, reusable energy storage.*

## **Introduction**

The Proton Exchange Membrane Fuel Cell (PEMFC) is very flexible in terms of its power and capacity requirements, its long-life service, good ecological balance and very low self-discharges [1].

PEMFC offers high power density, quick start-up and low operating temperatures as well as rapid response to varying operational loads in many applications [2]. Currently, a PEMFC with a net power density of 1kW/L has been achieved [3].

Air-cooled proton exchange membrane fuel cells (PEMFCs), combining air cooling and oxidant supply channels, offer a significantly reduced bill of materials and system complexity compared to the conventional, water-cooled fuel cells. In air-cooled PEMFC systems, ambient air is applied freely as the cooling medium which means that the cooling environment is highly influenced by the ambient temperature. High inlet air temperature would reduce the cooling efficiency.

Air-cooled fuel cell systems combine the cooling function with the cathode flow field and reduce overall cost by eliminating a lot of auxiliary systems required for conventional fuel cell designs (water cooling loop, air compressor and humidifier) [4].

Operation of a proton exchange membrane fuel cell (PEMFC) is a complex process that includes electrochemical reactions coupled with transport of mass, momentum, energy and electricity [5].

The operating conditions for the best performance require a balance between temperature, humidity and reactant flow rates in order to avoid flooding of electrodes [6]. The sensitivity of PEM fuel cell stacks to temperature is mainly related to the required moisture levels in the membrane that is hydrated from water back-diffusion flux from the cathode to the anode. When the operating current density increases, the effects of temperature on membrane hydration decrease slightly.

However, heat is also needed for improved reaction kinetics at the catalyst layers. The effects of the heat to the operation of a fuel cell are subjective and complex. Heat is needed to improve the reaction kinetics, but too much heat would lead to an increase in energy losses [7]. Therefore, thermal management of PEM fuel cells needs to balance delicately with both requirements.

The Proton Exchange Membrane Fuel Cell (PEMFC) is very flexible in terms of power and capacity requirements, its long-life service, good ecological balance and very low self-discharges [4].

Temperature is a crucial parameter for PEM fuel cell performance which directly or indirectly affects the reaction kinetics, transport of water, humidity level, conductivity of membrane, catalyst tolerance, removal of heat or thermal stresses in the membrane etc [4].

To conclude, the performance of the fuel cell increases as the temperature increases from room temperature to 80°C, further increase in temperature results in a current density dependent performance. The best performance was observed at around 80°C with 3 bars of absolute back pressure and 100% relative humidity.

For small size and performance of stacks (below 100W), the cooling can be achieved only with cathode air flow. A disadvantage here is that it requires relatively bigger channel size for cathode side of the stack compared with the anode side which consequently increases the volume of the stack. Stacks bigger than few hundred watts require a separate cooling channels.

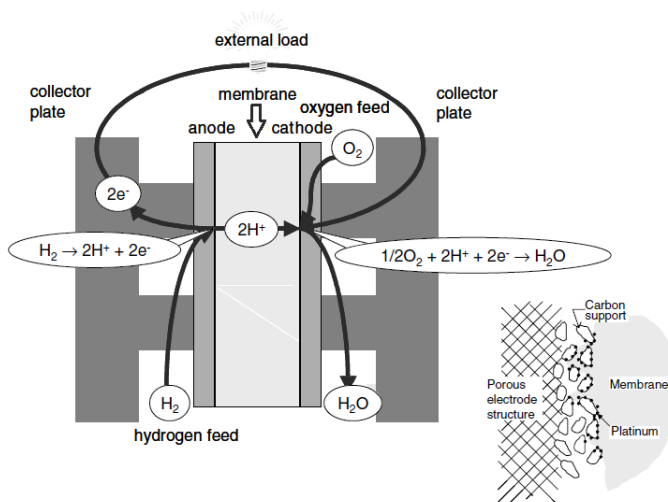


Fig.1. The basic principle of operation of a PEM fuel cell Source: [4].

## 1 Heat sources in PEMFC

The electrical performance of a PEM fuel cell dictates the generated thermal energy within the stack. The theoretical power curve of a fuel cell can be obtained by establishing electrochemical models based on the Nernst equation and subsequent voltage losses within the stack. Higher voltage losses at a specified current density lead to a higher heat generation. During the operation of a PEMFC, hydrogen molecules are supplied at the anode and split into protons and electrons. The polymeric membrane conducts protons to the cathode while the electrons move from anode to cathode through an external load powered by the cell. Oxygen (from air) reacts with the protons and electrons in the cathode half-cell where water and heat are produced.

The overall reaction of a PEM fuel cell is:



The electrical power ( $P_{el}$ ) is the desired system output and the stack heat generated, or thermal power ( $P_{th}$ ), of a fuel cell are linked through the actual output cell voltage ( $E_{cell}$ ) [7],

$$P_{el} = E_{cell} I_{FC} \quad (1)$$

where:  $I_{FC}$  is the current output, [A],

$$P_{th} = (E_{Nernst} - E_{cell}) I_{FC}, \quad (2)$$

where:  $E_{Nernst}$  is the maximum achievable (reversible) voltage of a fuel cell, [V],

$$E_{cell} = E_{Nernst} - E_{act} - E_{ohm} - E_{conc}, \quad (3)$$

where:  $E_{act}$  is activation,  $E_{ohm}$  is ohmic,  $E_{conc}$  is mass concentration cell energy loss.

The Nernst equation for the PEM fuel cell is [4]:

$$E_{Nernst} = -\frac{\Delta G}{nF} = -\frac{\Delta H - T_{FC} \Delta S}{nF} = -1.129 - \frac{RT_{FC}}{nF} \left[ \ln(p_{H_2}) + \frac{1}{2} \ln(p_{O_2}) \right] \quad (4)$$

where:  $\Delta H$  is the free reaction enthalpy at 298 K, which is 237.3 kJ/mol,  $\Delta S$  is the reaction entropy at 298 K which is 163.33 J/(K.mol) [7],  $n$  is the number of moles of electron transferred in the fuel cells reaction,  $F$  stands for Faradays constant (96,485 C/mol),  $T_{FC}$  is the fuel cell operating temperature, usually in the range of 50 °C–100 °C,  $p_{H_2}$  is the supply pressure of the hydrogen reactant into the stack [atm],  $p_{O_2}$  is the partial pressure of oxygen supply which is 0.21 atm for an intake of air at 1 atm [7].

### 1.1 Cell energy losses

The main energy loss is contributed by the activation over voltage which is the energy loss due to the activation of electrochemical reactions at the anode and cathode. Activation losses are caused by the slow onset of both anode and cathode reactions. Activation losses increase with current density and can be expressed using the Tafel equation [4].

$$E_{act} = \frac{RT_{FC}}{nF} \ln\left(\frac{i_{FC}}{i_o}\right), \quad (5)$$

where:  $R$  is the universal gas constant, [J/(K.kg)],  $T_{FC}$  is actual cell temperature [K],  $i_{FC}$  is generated current density, [A/cm<sup>2</sup>],  $i_o$  is a current density at electrode equilibrium [A/cm<sup>2</sup>].

The second type of energy loss is Ohmic loss contributed by the resistance to charge flow within the cell and can be represented using Ohm's law [4].

$$E_{ohm} = I_{FC}(R_{electrodes} + R_{membrane}) \quad (6)$$

where:  $R_{electrodes}$  is resistance of electrodes (resists electron flow), [Ω],  $R_{membrane}$  is resistance of membrane (resistance to proton flow through the membrane), [Ω].

The conductivity of the electrodes decreases with increasing temperature of the FC. With the increase of the temperature, the resistance of the membrane decreases. The resistance of the membrane dominates over the resistance of electrodes. The membrane resistance can be determined from the following relationship [5]:

$$R_{membrane} = \frac{r_m L_m}{A} \quad (7)$$

where:  $r_m$  is the specific resistivity of the membrane to electron flow, [Ω.cm],  $L_m$  is the thickness of the membrane, [cm],  $A$  is the active area of the PEM fuel cell, [cm<sup>2</sup>].

The concentration losses can be calculated by

$$E_{conc} = \frac{RT_{FC}}{nF} \ln\left(\frac{i_L}{i_L - i_{FC}}\right) \quad (8)$$

where:  $i_L$  is the maximum current density of the FC, [A/cm<sup>2</sup>],  $i_{FC}$  is the actual current density, [A/cm<sup>2</sup>].

The voltage values at a certain current density can be obtained by measuring the polarization curve of the PEM fuel cell. These values serve as an input in simulation model based on equation (5), (6), (7) and (8). The simulation model was created in MATLAB.

As the values obtained show, activation losses have the biggest influence on the output voltage of the PEM fuel cell. It is possible to decrease these values by increasing the charge transfer coefficient  $\alpha$ , increasing the kinetics of electrode reactions, increasing exchange current density  $i_o$ , and by decreasing partial pressures and temperatures of reaction gases.

Concentration losses at a high current density have a significant influence. These losses can be limited by maintaining the consumption rate of reaction gases under the value of diffusion coefficient  $D$ . The diffusion coefficient defines the rate of movement as the substance diffuses into the environment, the movement being a response to the concentration gradient in the medium in which the substance is. In order to achieve this condition, it is necessary to change the geometry of cells or decrease current density. Last but not least, there are also ohmic losses which grow almost linearly with increasing current density. However, limiting ohmic losses is more complicated since they can be limited only by using materials with lower electrical resistance. Here the reaction rate of reaction gases must be taken into consideration when using different material as it can have a significant influence on increasing other voltage losses.

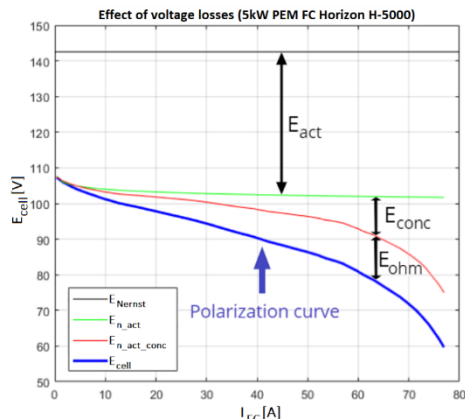


Fig.2. Effect of individual voltage losses on value of the resulting generated voltage.

After calculating individual voltage losses, the figures are used to determine the resulting PEM fuel cell voltage so that the gradual change of generated voltage under the influence of individual losses can be seen. shows the effect of individual voltage losses on generated voltage.

The significant voltage decrease at low current density is caused both by internal currents and by fuel transfer from cathode to anode. These losses are a result of short circuit in electrolyte and transfer of reactants through electrolyte. Although the electrolyte of fuel cell serves as a transfer of ions in the first place, it is not entirely isolated from electrones and will therefore be always able to let a very small amount of electrones through. This ability presents a net loss against/towards an outer circuit. In a real fuel cell, the diffusion process will cause that some of the reactants will move from one electrode to another one through electrolyte where it will react without electrone transfer through the external circuit.

(Fig.2) shows four dependences of output voltage  $E_{FC}$  as a function of current load  $I_{FC}$  in measured Horizon H-5000 PEM fuel cell. Individual voltage losses are gradually added to the polarization curve of the ideal (Nernst) output voltage  $E_{Nernst}$ .

The polarization curve marked as  $E_{Nernst}$  shows the progress of ideal (Nernst) output voltage. The curve marked as  $E_{n\_akt}$  points to the progress of output voltage taking activation losses  $E_{act}$  into consideration. The curve marked as  $E_{n\_akt\_conc}$  shows output voltage polarization curve including activation  $E_{act}$  and concentration  $E_{conc}$  losses. The polarization curve marked as  $E_{cell}$  represents the measured values of the PEM fuel cell output voltage.

Table 1. Comparison of output voltage values when considering individual losses at different current density values.

Parameter	$E_{Nernst}$ [V]	$E_{n\_akt}$ [V]	$E_{n\_akt\_conc}$ [V]	$E_{cell}$ [V]
$I_{FC\_L}$	142.56	107.9	107.4	107.3
$I_{FC\_M}$	142.56	102.7	100.3	94.3
$I_{FC\_H}$	142.56	101.9	85.8	71.8

In order to compare the changes of output voltage, three current load values were chosen in (Tab. 1). Low current load  $I_{FC\_L}$  equals 0.35 [A], medium current load  $I_{FC\_M}$  equals 33.41 [A] and high current load  $I_{FC\_H}$  equals 70 [A]. (Fig.2) also pictures maximum current load of Horizon H-5000 PEM fuel cell. It is the so called maximum current density which is characterized by insufficient amount of reaction gases on the surface of the catalyst.

Every fuel cell has a maximum of current density called as limiting current density of FC. The limit of this values is 76.93 [A] when measuring on Horizon H-5000 PEM fuel cell.

## 1.2 Heat generation

All the chemical energy that we have available in a fuel cannot be converted into useful work (electrical energy) because of the enthalpy (entropy) change during a chemical reaction. The heat generated within fuel cells is assumed to be the heat generated mainly at the electrochemical reaction sites of the cathodes. Generally, to determine the amount of heat produced by a fuel cell, an energy balance for a fuel cell stack can be provided:

$$\sum_i H_{i,in} = \sum_i H_{i,out} + P_{el} + \dot{Q}_{gen}, \quad (9)$$

or:

$$\dot{Q}_{gen} - \Delta H_i + P_{el} = 0, \quad (10)$$

where:  $H_{i,in}$ ,  $H_{i,out}$  are the enthalpies of reactants and products [kJ/kmol],  $P_{el}$  is the electrical power generated by the fuel cell [W],  $\dot{Q}_{gen}$  is heat generated by the fuel cell, [W].

The amount of heat generated can be estimated using the simplified relations based on the energy balance of the system and depending on the state of water formed [7]:

$$\frac{I_{FC}}{nF} H_u n_{cell} = I_{FC} E_{cell} n_{cell} + \dot{Q}_{gen}, \quad (11)$$

where:  $H_u$  is low heating value of hydrogen [kJ/kg].

If the water exists as vapor at room temperature, then the  $E_{Nernst}$  voltage is 1.254 [V] and the stack thermal power  $P_{th}$  is dependent on the current produced and cell voltage [5]:

$$\dot{Q}_{gen} = P_{th} = (E_{Nernst} - E_{cell}) I_{FC} n_{cell} \quad (12)$$

A fuel cell stack may dissipate its heat energy by internal as well as external mechanisms. Internal heat removal by the cathode fluid stream is more significant than the anode fluid stream as the exothermic reactions occur at the cathode and produced water absorbs the generated heat.

A simple way to improve the performance of a fuel cell is to operate the system at its maximum allowed temperature. At higher-temperature, the electrochemical activities increase, and the reaction takes place at a higher rate, which in turn increases the power output. On the other hand, operating temperature affects the maximum theoretical voltage at which a fuel cell can operate. Higher temperature corresponds to lower theoretical maximum voltage and lower theoretical efficiency. Temperature in the cell also influences cell humidity which significantly influences membrane ionic conductivity.

Therefore, temperature has an indirect effect on the cell performance through its impact on the membrane water content. The durability of the membrane electrolyte is another barrier for higher-temperature operation due to performance degradation during long-term operation. Scientists analyzed electrochemical performances as a function of the temperature distribution.

## 2 Analytical Simulation Model of PEMFC Stack

From the governing equations discussed before, an analytical zero-dimensional dynamic simulation model was created in *Matlab Simulink* environment. Topological diagram of the created simulation model can be seen in (Fig.3). The model consists of three interconnected subsystems which are responsible for simulating electrochemical, thermodynamic and mass transport effects that occur within the fuel cell stack. With this model, it's possible to analyze the effects of ambient and operating conditions on generated output power of the used fuel cell stack in steady state and transient modes of operation [10], [11].

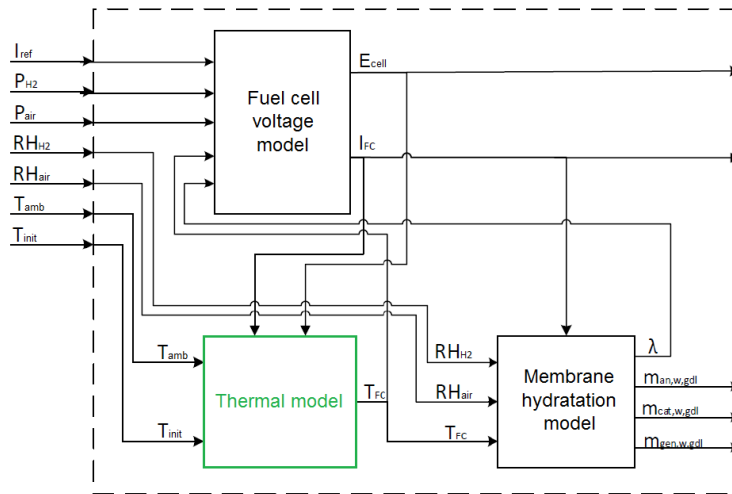


Fig.3. Topological diagram of PEMFC simulation model [10], [11].

### Input parameters of the model:

$I_{ref}$	– load current (reference current) [A]
$P_{H_2}$	– pressure of the hydrogen [atm]
$P_{air}$	– pressure of the ambient air [atm]
$RH_{H_2}$	– relative humidity of the hydrogen [%]
$RH_{air}$	– relative humidity of the ambient air [%]
$T_{amb}$	– temperature of the ambient air [°C]
$T_{init}$	– initial temperature of the FCS [°C]

### Output parameters of the model:

$E_{cell}$	– generated voltage of the fuel cell [V]
$I_{FC}$	– generated current of the fuel cell [A]
$m_{an,w,gdl}$	– amount of water transferred from membrane to anode GDL [l]
$m_{cat,w,gdl}$	– amount of water transferred from membrane to cathode GDL [l]
$m_{gen,w,gdl}$	– total amount of generated water [l]

### Internal parameters of the model:

$\lambda$	– relative water content in the membrane [-]
$T_{FC}$	– actual working temperature of the FC [°C]

The following assumptions are made for the created analytical model [9], [11]: (1) The reacting gases are considered to be ideal; (2) The temperature is same in all parts of the fuel cell stack i.e. the effect of conduction heat transfer is neglected; (3) No pressure drops across the flow channels are considered; (4) The flow of generated water and reacting gases through membrane is not considered; (5) thermodynamic properties of the solid phase are constant; (6) due to relatively low temperature and surface area exposed to radiation, the radiation heat transfer is neglected; (7) the relation between heat generation and local current density is linear. The focus of this paper is the thermal analysis of the PEMFC and therefore, the thermal subsystem highlighted with green color in the (Fig.3) will be further discussed in detail.

## 2.1 Thermal model of PEMFC stack

The thermal model of PEM fuel cell stack describes the changes of stack temperature depending on the ambient temperature, heat generated by occurring electrochemical reactions and the heat dissipated from the fuel cell by active or passive cooling. (Fig.4) shows the block representation of the PEMFC thermal model as a MISO system with corresponding inputs and outputs. The generated fuel cell output current  $I_{FC}$  and voltage  $E_{cell}$  which are both results from electrochemical reactions, ambient temperature  $T_{amb}$  and initial temperature of the fuel cell stack are considered as inputs to the system. The only output of the system is the fuel cell stack actual temperature  $T_{FC}$  [10], [11].

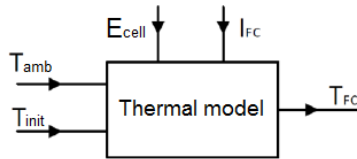


Fig.4. Block representation of PEMFC thermal model.

The transient change in fuel cell temperature can be represented by the following first order differential equation [8], [10], [11]:

$$\frac{dT_{FC}}{dt} = \frac{\Delta\dot{Q}}{M_{stack}c_{stack}}, \quad (13)$$

where  $\Delta\dot{Q}$  represents a total heat flow inside the fuel cell stack [W],  $M_{stack}$  is a weight of the fuel cell stack [kg] and  $c_{stack}$  is an average heat capacity of the fuel cell stack [J/(K.kg)].

The total heat flow of the fuel cell stack can be calculated as a difference between generated and dissipated heat at any given time by equation [8]:

$$\Delta\dot{Q} = \dot{Q}_{gen} - \dot{Q}_{diss}, \quad (14)$$

where  $\dot{Q}_{gen}$  is the generated heat flow [W] and  $\dot{Q}_{diss}$  represents the heat dissipated from the fuel cell stack [W].

According to the fourth mentioned equation, the value of the total heat flow will be positive when the temperature of the system is rising and negative when the temperature is decreasing. Its value can be also considered as a global heat gradient of the system. The amount of generated heat flow  $\dot{Q}_{gen}$  depends on the number of exothermic and endothermic electrochemical reactions occurring during the fuel cell operation as seen in (12), [9], [10], [11].

The generated heat is causing an increase in fuel cell temperature, which in long enough time can reach values outside the operating temperature range of PEMFC. To maintain desired operating temperature of the stack, part of generated heat must be dissipated from the stack. Dissipation of heat from the considered air-cooled DEA PEMFC is caused by cooling system represented by cooling fan and by natural heat transfer mechanisms, namely convection and conduction heat transfer.

The equation of dissipated heat flow can be written as [10]:

$$\dot{Q}_{diss} = \dot{Q}_{fan} + \dot{Q}_{nat.conv}, \quad (15)$$

where  $\dot{Q}_{fan}$  is a heat flow dissipated by the cooling fan [W] and  $\dot{Q}_{nat.conv}$  is a heat flow dissipated from the surface of the FCS by natural convection [W]. The dissipation of heat by conduction heat transfer mechanism is not considered for the created model.

The following expression can be written for the heat flow dissipated by the cooling fan [8], [11]:

$$\dot{Q}_{fan} = \dot{m}_{air} c_{p,air} (T_{air,out} - T_{amb}), \quad (16)$$

where  $\dot{m}_{air}$  is a mass flow rate of air [kg/s],  $c_{p,air}$  is a specific heat capacity of the air [J/(K.kg)],  $T_{air,out}$  is a temperature of the air exiting the cathode channels [°C]. The mass flow rate of air is generally dependent on stoichiometry coefficient of the air and generated output power of the FCS. Since there is no temperature regulation implemented in the model, the air mass flow rate  $\dot{m}_{air}$  will be considered constant and its value is given by the amount of air flowing into system through the cooling fan [10], [11]. For the used PEMFCS and other small FCS, it can be assumed that the temperature of exiting cathode air  $T_{air,out}$  is equal to the actual fuel cell temperature  $T_{FC}$  [11].

Heat flow dissipated by means of the natural convection from the FCS surface is given by following relation [8], [11]:

$$\dot{Q}_{nat.conv} = \alpha_{conv} A_{stack} (T_s - T_{amb}), \quad (17)$$

where  $\alpha_{conv}$  is a coefficient of convection [W/(K.m<sup>2</sup>)],  $A_{stack}$  is the outer surface area of the FCS [m<sup>2</sup>] and  $T_s$  represents the temperature of the surface area [°C], which is in considered model, equal to FCS actual temperature  $T_{FC}$ . For laminar flow of air, the convection coefficient for heat transfer from fuel cell stack surface to the ambient air reaches values from 5 to 10 W/(K.m<sup>2</sup>) [11].

The complete simulation model of the thermal subsystem which was created utilizing the equations (13) – (17) can be seen in (Fig.5). Values of the required constants of the model are summarized in (Tab.2).

## 3 Results and Discussion

### 3.1 Model validation

In order to validate the performance of the created analytical simulation model with the experimental data obtained from real laboratory fuel cell stack, an experimental work station shown in (Fig.6) had to be constructed. The main part of the station is a commercial air-cooled PEM fuel cell stack Horizon H-12 which is labelled (1) in (Fig.6). Basic parameters for this FCS datasheet are shown in (Tab.3).

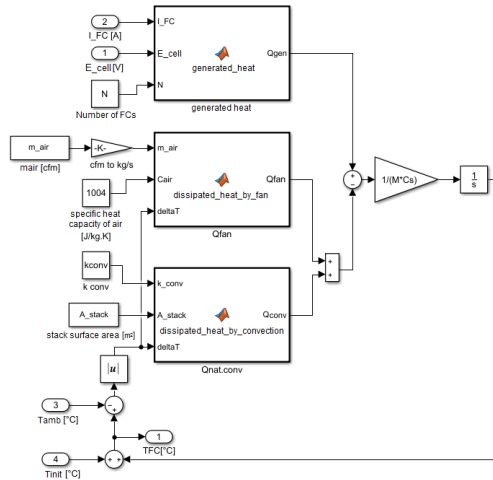


Fig.5. Simulation model - thermal subsystem [10].

Table 2. Simulation parameters of the model [11].

Sign	Name	Value	Unit
$M_{stack}$	Weight of the FCS	0.25	[kg]
$c_{stack}$	Average heat capacity of FCS	50	[J/(K.kg)]
$E_{Nernst}$	Theoretical (Nernst) voltage of PEMFC	1.229	[V]
$\dot{m}_{air}$	Mass flow rate of air	4	[g/s]
$c_{p,air}$	Specific heat capacity of air	1004	[J/(K.kg)]
$T_{amb}$	Temperature of ambient air	25	[°C]
$T_{init}$	Initial temperature of FCS	25	[°C]
$\alpha_{conv}$	Coefficient of natural convection	7	[W/(K.m²)]
$A_{stack}$	Outer surface area of FCS	42	[cm²]

Second part of the station are two metal-hydride Hydrostick cartridges (2) which can hold up to 10Wh of energy each, stored in 10L of pure dry hydrogen. The cartridges are connected to the FCS via a one-way pressure regulating valves which are used to reduce the pressure of the cartridges to FCS input pressure of 0.5bar. To ensure the desired functionality of the work station, a commercial control unit supplied with the FCS was replaced by control unit (4) which was created by one of our students as a part of his diploma thesis [11].

The control unit is able to measure voltage and current of the FCS and also humidity and temperature of the ambient air. These values are transferred to the PC (5) by a USB interface for validation and visualization in MATLAB environment. Besides that, the control unit also generates a load to the FCS with the use of a controlled power MOSTFET transistor. Last functions of the control unit are the ability to short circuit the outputs of FCS and to operate the purging valve (3). The Arduino NANO was chosen as a microprocessor for this control unit [11].

Using the described work station, we measured the polarization curve of the fuel cell stack, which is a standard characteristic curve for the fuel cells. It represents a steady state characteristic of fuel cell voltage degradation in the whole operating range of the generated output current [10].

The measured data were then scaled down to represent a polarization curve for single fuel cell. Comparison between the measured and simulated curves is displayed in (Fig.7).

The degradation occurs mainly due to polarization losses as described in 1.1. From the character of the curves, it is clear that they correlate well in the center region where the ohmic losses are dominant.

Good fit of model in this region is important because most of fuel cells are operated in the region of ohmic losses due to presence of their peak power point. Larger deviation is observed in the regions of activation and mass transport losses where the model shows more pronounced logarithmic character than the measurement.

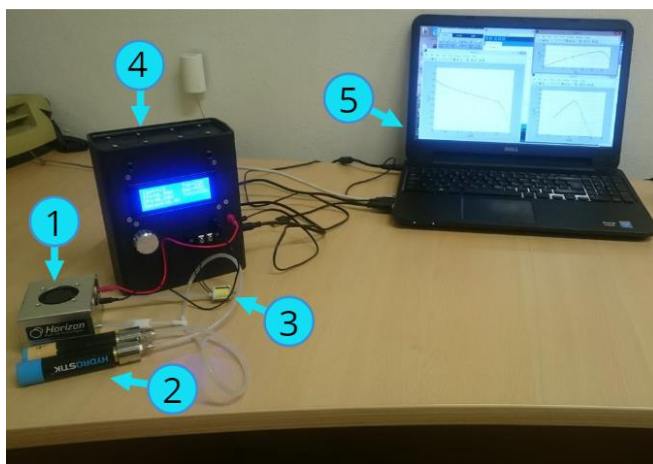


Fig.6. Experimental work station.

Table 3. Basic parameters of Horizon H-12 [12].

Parameter	Value
Number of fuel cells	13
Nominal power	12W (7.8V and 1.5A)
Maximum operating temperature	55°C
Input pressure of hydrogen	0.45 - 0.55bar
Desired hydrogen purity	at least 99.995%
Membrane humidification	self-hydrated
Cooling method	Integrated cooling fan
Weight of the FCS	275 ± 30g
FCS dimensions	7.5 x 4.7 x 7 cm
Flow rate of the hydrogen at maximum load	0.18 l/min
Efficiency at nominal power	40%

In (Fig.8) the power curves of model and measurement are compared. The slopes of the curves correlate very well. The main difference is visible at the peak power point where the shape of the curves differs. This deviation is caused by different character of the polarization curves between model and measurement in the region where the concentration losses are dominant. This can be seen in (Fig.7) where, upon entering the concentration losses region, the measured polarization curve decreases much faster than the simulated curve which resembles its theoretical logarithmic shape.

The nominal power of the FCS that the manufacturer states in the datasheet is 12W but from the measured values in (Fig.8) we can see that the peak power of used FCS can reach values up to 15.5W in the concentration losses region.

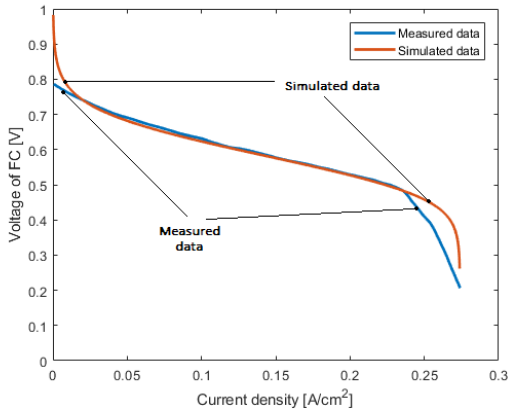


Fig.7. Comparison of measured and simulated polarization curve.

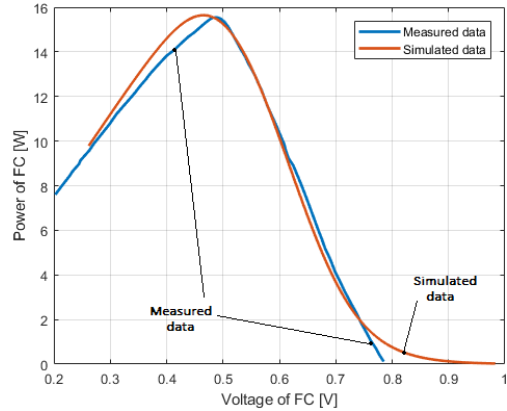


Fig.8. Comparison of power curves from measurement and simulation.

### 3.2 Simulation results

With validated simulation model we proceeded to analyze the effects of temperature variations on fuel cell performance. (Fig.9) shows the relation between fuel cell temperature and its theoretical (Nernst) voltage in various constant pressure conditions. It is clear that the theoretical voltage is decreasing with temperature.

This decrease in voltage is caused by the expansive property of reactant gasses. Increase in temperature is causing the gasses to expand which in turn leads to lower concentration of reactant molecules on the surface of the electrodes. This means that less redox reactions occur on the electrodes which decreases the fuel cell output voltage.

From the (5) – (8) it is clear that the temperature also influences all three voltage overpotentials. Effect of temperature on activation losses is shown in (Fig.10). We can see that the activation losses are increasing in value along with the rising temperature. From (Fig.11) we can see that the relationship is strictly linear. This linear relation also applies to the concentration losses.

The effect of temperature on concentration losses can be seen in (Fig.12). The change of concentration losses due to change in temperature is very minimal. Dominant changes are visible in the convex region of the depicted curves.

In (Fig.13), the effect of temperature on ohmic losses is shown. It can be seen that the temperature clearly has a significant effect on the slope of the curve. This decrease in slope is caused by the decrease of membrane resistance which is always bigger than the increase in electrical resistance of contacts and wiring to the load circuit.

The complex effect of temperature on FC losses can be seen on the polarization curves in (Fig.14). From the character of the curves, we can see that the increase in temperature lowers the value of theoretical voltage as shown in (Fig.9). On the other hand, the higher temperature causes an increase in FC voltage in higher current densities. This is caused by the fact that the effect of lowering ohmic losses is more significant than the negligible increase in concentration losses. Since the peak power operating point also falls into the region of high current densities, increasing the temperature also rises the overall power output of the FCS which can be seen in (Fig.15).

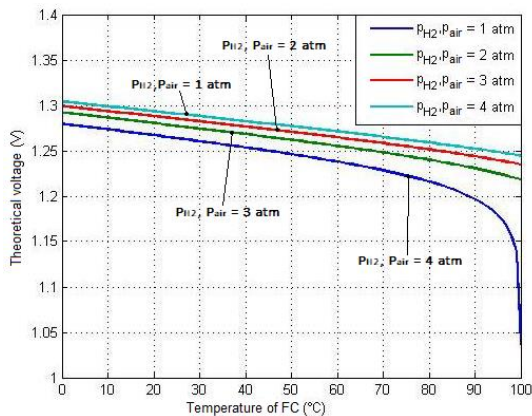


Fig.9. Theoretical voltage as a function of temperature at constant pressure conditions [11].

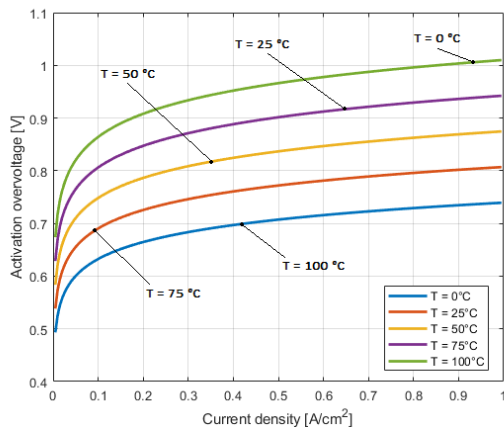


Fig.10. The effect of temperature on the character of activation losses.

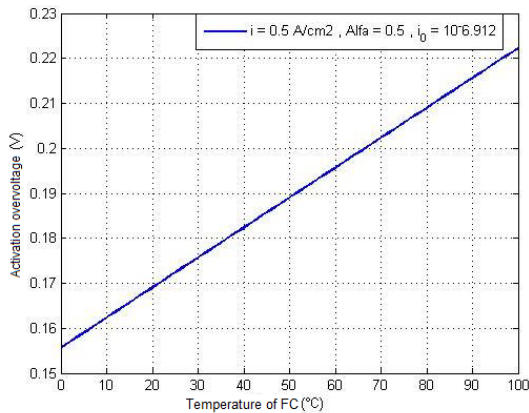


Fig.11. Relationship between activation losses and temperature at fixed current density [11].

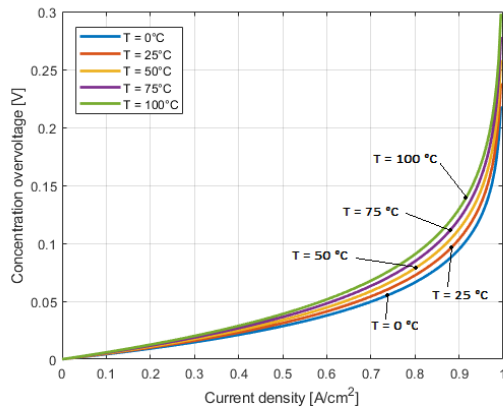


Fig.12. The effect of temperature on the character of concentration losses.

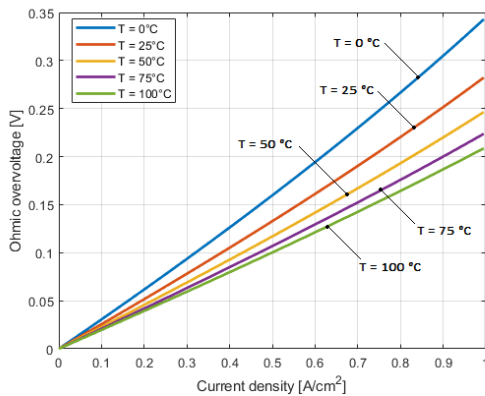


Fig.13. The effect of temperature on the character of ohmic losses.

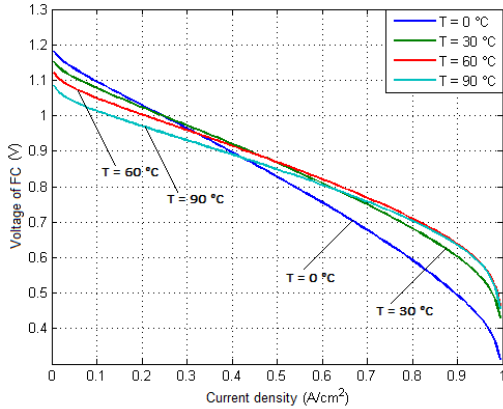


Fig.14. The effect of temperature on the character of polarization curve [11].

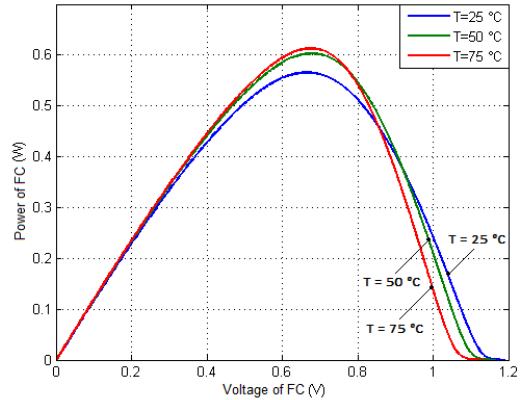


Fig.15. The effect of temperature on the value of power output [11].

The biggest change is achieved in the region of maximum peak power at voltages from 0.6 to 0.8V. Increase in the maximum power of the PEMFC is limited by the boiling point of water. From the relation between maximum power and temperature in (Fig.16) we can see that the optimal temperature range for obtaining maximum possible power is from 60 to 80°C. Efficiency of the FC is also influenced by temperature. In (Fig.17), the relation between efficiency and power density of PEMFC is displayed.

The efficiency decreases with current density substantially. Once the power density reaches its maximum, any further increase in current density will lead to decrease in both efficiency and power density. This is the region of mass transport losses where the PEMFCs are not supposed to be used. The increase in temperature is causing a slight loss of efficiency in the region of low current densities where the efficiency reaches its maximum values.

On the contrary, in the region of high current densities, the efficiency of the stack increases. This is caused by shifting of the maximum power operating point towards higher values of output current density and voltage.

In order to analyze dynamical properties of temperature and heat flow of the created thermal model, we carried out simulation of a transient response of FC the heat flow and temperature to the dynamic changes of generated electrical power.

In (Fig.18) we can see that the temperature of the FC increases almost linearly after the positive step change in electrical power at the time of 3s. When the generated power is decreased in two subsequent steps at the times of 5 and 7s, we can see that the temperature starts to decrease with much slower exponential character. This shows that the temperature increase by heat generation has much faster dynamics than the temperature decrease caused by cooling mechanisms.

In (Fig.19), the response of the heat flow and its components to the power profile from (Fig.18) is depicted. It is clear that the cooling fan has a major contribution to the heat dissipation from the FCS. In comparison, the heat dissipated from the FC surface by the effect of natural convection is negligible. This fact stresses the importance of implementing correct cooling systems with adequate temperature regulation for maintaining desired operation temperature range of used FC system. It is also worthy to note that in the mobile applications, the cooling system is usually responsible for the significant part of energy consumption of the system.

We can also see that since the mass flow rate of inlet air is constant, the character of  $\dot{Q}_{fan}$  closely resembles the character of temperature transient response in (Fig.18) as its expected from the governing equation (16). The resemblance between the  $\dot{Q}_{nat.conv}$  transient and the temperature transient is also very strict given the equation (17) but due to small values of  $\dot{Q}_{nat.conv}$  and scale used in (Fig.19) it is not visible.

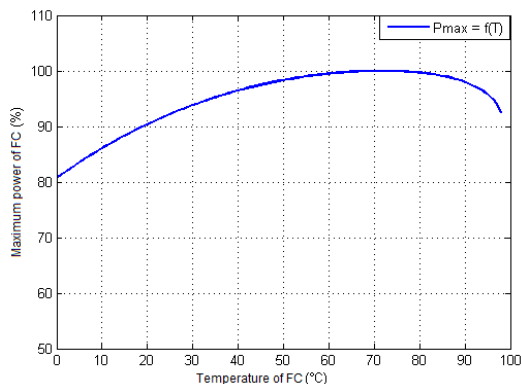


Fig.16. Maximum power of FC as a function of temperature [11].

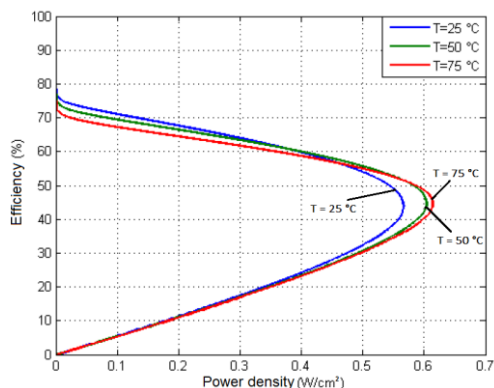


Fig.17. Efficiency of the FC as a function of power density [11].

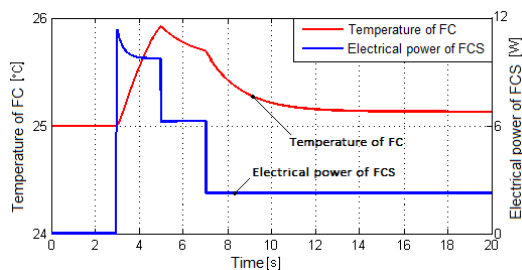


Fig.18. Transient response of the temperature to dynamic power profile.

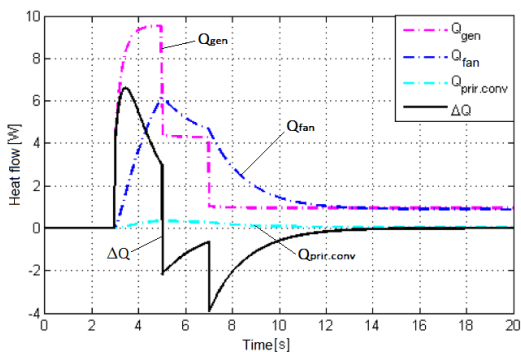


Fig.19. Transient response of the heat flow and its components to the dynamic power profile.

## Conclusion

This paper is focused at analysing temperature effects on the performance of a small-scale commercial PEM fuel cell stack. The Horizon H-12 air cooled PEMFCS with dead-ended anode was used. For the purpose of analysing the effects of temperature on various parameters of PEMFCS in steady state and transient conditions without a need of experiments, an analytical zero-dimensional dynamic model was developed and validated to experimental data. The model is able to simulate electrochemical, thermodynamic and mass transport properties of the FCS. Regarding the scope of this paper, only thermal model was discussed in detail.

The temperature effects on FCS polarization curve as well as on the power and efficiency curves of the stack were observed. Changes in individual voltage overpotentials and theoretical Nernst voltage were also evaluated. Our analysis shows that the temperature increase influences the activation losses the most, significantly increasing their value. On the contrary, ohmic losses are reduced which in turn causes an increase of nominal power output of the stack. The effect on concentration losses is negligible.

Efficiency of the stack exhibits a decrease in value at low current densities and increase at high current densities when the temperature rises.

The maximum output power to temperature relation proved that the optimal temperature range for obtaining maximum power for the used PEMFCS is 60-80°C as stated by literature. Dynamic behaviour of temperature and heat flow in reaction to load variations shows the dominance of forced convection in heat dissipation of the stack and stresses the importance of implementing auxiliary cooling systems to maintain required operational temperature.

In our future work we will explore the influence of heat generation on water production and humidity inside the FCS which are highly interconnected effects. This intention requires consideration of the following aspects:

- In addition to supplying the reactants to the fuel cell stack, the fuel cell system must also take care of the fuel cell by products – water and heat.
- Water is essential for proton transport across the polymer membrane. Water must be collected at the fuel cell exhaust for reuse.
- On a system level, including hydrogen and oxygen storage tanks, the mass of the system does not change, that is, hydrogen and oxygen are converted to water.
- The same water may be used for humidification and to remove the heat from the stack. Heat is discharged from the system through a radiator or a liquid heat exchanger.

## References

- [1] KAMARUDIN S.K., DAUD W.R.W, YAAKUB Z., ANUAR W., YUSUF N.N.A.N. and MISRON Z., *Synthesis and optimization of future hydrogen energy infrastructure planning in Peninsular Malaysia*, in Int. J. Hydrogen Energy, 2009, 34, 2077-88.
- [2] SQUADRITO G., BARBERA O., GIACOPPO G., URBANI F. and PASSALACQUA E., *Polymer electrolyte fuel cell stack research and development*, in Int. J. Hydrogen Energy, 2008, 33, 1941-6
- [3] BASCHUK J. and LI X., *Comprehensive, consistent and systematic mathematical model of PEM fuel cells*, in Appl. Energy, 2009, 86, 181-93.
- [4] BARBIR F., *PEM Fuel Cells – Theory and Practice*, Elsevier – Academic press, 2005, ISBN 978-0-12-078142-3.
- [5] LARMINIE J. and LOWRY J., *Electric Vehicle Technology Explained*, John Willey & Sons, Ltd, 2003, ISBN 0-470-85163-5.
- [6] MILLERA M. and BAZYŁAKA A., *A review of polymer electrolyte membrane fuel cell stack testing*, in J. Power Sources 2011, 196, 601-13.
- [7] MOHAMED W.A. and ATAN R., *Experimental thermal analysis on air cooling for Polymer Electrolyte Membrane fuel cells*, in Int. J. Hydrogen Energy, 2015, 40, 10605-10626.
- [8] LISO V., NIELSEN M. P., KÆR S. K. and MORTENSEN H. H., *Thermal modeling and temperature control of a PEM fuel cell system for forklift applications*, in International Journal of Hydrogen Energy, Elsevier, 2014, pp. 8410-8420
- [9] SHAHSAVARI S., DESOUZA A., BAHRAMI M. and KJEANG E., *Thermal analysis of air-cooled PEM fuel cells*, in International Journal of Hydrogen Energy, Elsevier, 2012, pp. 18261-18271
- [10] FERENCEY V., *Sources and reservoirs of electrical energy for mobile means (sk. Zdroje a zásobníky elektrickej energie pre mobilné prostriedky)*, Slovakia: STU Bratislava, 1st ed., 2016, pp. 76-110, ISBN: 978-80-89597-51-2
- [11] GALOVIČ M., *PEM fuel cell power control*, Diploma thesis, Slovakia: FEI STU Bratislava, 2015, pp. 27-29, 35-53, 63-68
- [12] HORIZON FUEL CELL TECHNOLOGIES, *Horizon H-12 Fuel Cell Stack User Manual*, ver. 2.4, Dec. 2011 pp. 11-12

## ▲ Authors



**Prof. Ing. Viktor Ferencey, PhD.**

Department of Automotive Mechatronics  
Faculty of Electrical Engineering and Information Technology  
Slovak University of Technology, Bratislava, Slovakia  
viktor.ferencey@stuba.sk

**Ing. Michal Stromko**

Department of Automotive Mechatronics  
Faculty of Electrical Engineering and Information Technology  
Slovak University of Technology, Bratislava, Slovakia  
michal.stromko@stuba.sk



**Ing. Kristián Ondrejčka**

Department of Automotive Mechatronics  
Faculty of Electrical Engineering and Information Technology  
Slovak University of Technology, Bratislava, Slovakia  
kristian.ondrejicka@stuba.sk

